Research Article | Vol. 26, No. 15 | 23 Jul 2018 | OPTICS EXPRESS 19059
Optics EXPRESS

Ultrabroadband etalon-free detection of infrared transients by van-der-Waals contacted sub-10-µm GaSe detectors

MATTHIAS KNORR, PHILIPP STEINLEITNER, JÜRGEN RAAB, IMKE GRONWALD, PHILIPP MERKL, CHRISTOPH LANGE, AND RUPERT HUBER*

Department of Physics, University of Regensburg, 93040 Regensburg, Germany
**rupert.huber@ur.de*

Abstract: We demonstrate ultrabroadband electro-optic detection of multi-THz transients using mechanically exfoliated flakes of gallium selenide of a thickness of less than 10 µm, contacted to a diamond substrate by van-der-Waals bonding. While the low crystal thickness allows for extremely broadband phase matching, the excellent optical contact with the index-matched substrate suppresses multiple optical reflections. The high quality of our structure makes our scheme suitable for the undistorted and artifact-free observation of electromagnetic waveforms covering the entire THz spectral range up to the near-infrared regime without the need for correction for the electro-optic response function. With the current revolution of chemically inert quasi-two-dimensional layered materials, we anticipate that exfoliated van-der-Waals materials on index-matched substrates will open new flexible ways of ultrabroadband electro-optic detection at unprecedented frequencies.

OCIS codes: (320.7100) Ultrafast measurements; (120.5050) Phase measurement; (160.2100) Electro-optical materials; (230.2090) Electro-optical devices; (120.2230) Fabry-Perot.

References and links

1. R. Ulbricht, E. Hendry, J. Shan, T. F. Heinz, and M. Bonn, "Carrier dynamics in semiconductors studied with time-resolved terahertz spectroscopy," Rev. Mod. Phys. **83**(2), 543–586 (2011).
2. P. U. Jepsen, D. G. Cooke, and M. Koch, "Terahertz spectroscopy and imaging - Modern techniques and applications," Laser Photonics Rev. **5**(1), 124–166 (2011).
3. T. Kampfrath, K. Tanaka, and K. A. Nelson, "Resonant and nonresonant control over matter and light by intense terahertz transients," Nat. Photonics **7**(9), 680–690 (2013).
4. Q. Wu and X.-C. Zhang, "Ultrafast electro-optic field sensors," Appl. Phys. Lett. **68**(12), 1604–1606 (1996).
5. Q. Wu and X.-C. Zhang, "Free-space electro-optics sampling of mid-infrared pulses," Appl. Phys. Lett. **71**(10), 1285–1286 (1997).
6. A. Leitenstorfer, S. Hunsche, J. Shah, M. C. Nuss, and W. H. Knox, "Detectors and sources for ultrabroadband electro-optic sampling. Experiment and theory," Appl. Phys. Lett. **74**(11), 1516–1518 (1999).
7. R. Huber, A. Brodschelm, F. Tauser, and A. Leitenstorfer, "Generation and field-resolved detection of femtosecond electromagnetic pulses tunable up to 41 THz," Appl. Phys. Lett. **76**(22), 3191–3193 (2000).
8. C. Kübler, R. Huber, S. Tübel, and A. Leitenstorfer, "Ultrabroadband detection of multi-terahertz field transients with GaSe electro-optic sensors. Approaching the near infrared," Appl. Phys. Lett. **85**(16), 3360–3362 (2004).
9. K. Liu, J. Xu, and X.-C. Zhang, "GaSe crystals for broadband terahertz wave detection," Appl. Phys. Lett. **85**(6), 863–865 (2004).
10. T. Kampfrath, J. Nötzold, and M. Wolf, "Sampling of broadband terahertz pulses with thick electro-optic crystals," Appl. Phys. Lett. **90**(23), 231113 (2007).
11. M. Tonouchi, "Cutting-edge terahertz technology," Nat. Photonics **1**(2), 97–105 (2007).
12. S. Keiber, S. Sederberg, A. Schwarz, M. Trubetskov, V. Pervak, F. Krausz, and N. Karpowicz, "Electro-optic sampling of near-infrared waveforms," Nat. Photonics **10**(3), 159–162 (2016).
13. T. Seifert, S. Jaiswal, U. Martens, J. Hannegan, L. Braun, P. Maldonado, F. Freimuth, A. Kronenberg, J. Henrizi, I. Radu, E. Beaurepaire, Y. Mokrousov, P. M. Oppeneer, M. Jourdan, G. Jakob, D. Turchinovich, L. M. Hayden, M. Wolf, M. Münzenberg, M. Kläui, and T. Kampfrath, "Efficient metallic spintronic emitters of ultrabroadband terahertz radiation," Nat. Photonics **10**(7), 483–488 (2016).
14. R. Huber, F. Tauser, A. Brodschelm, M. Bichler, G. Abstreiter, and A. Leitenstorfer, "How many-particle interactions develop after ultrafast excitation of an electron-hole plasma," Nature **414**(6861), 286–289 (2001).
15. T. L. Cocker, D. Peller, P. Yu, J. Repp, and R. Huber, "Tracking the ultrafast motion of a single molecule by femtosecond orbital imaging," Nature **539**(7628), 263–267 (2016).

#330344 https://doi.org/10.1364/OE.26.019059
Journal © 2018 Received 26 Apr 2018; revised 15 Jun 2018; accepted 19 Jun 2018; published 12 Jul 2018

Optics EXPRESS

16. M. Hohenleutner, F. Langer, O. Schubert, M. Knorr, U. Huttner, S. W. Koch, M. Kira, and R. Huber, "Real-time observation of interfering crystal electrons in high-harmonic generation," Nature **523**(7562), 572–575 (2015).
17. M. Porer, J.-M. Ménard, and R. Huber, "Shot noise reduced terahertz detection via spectrally postfiltered electro-optic sampling," Opt. Lett. **39**(8), 2435–2438 (2014).
18. I.-C. Benea-Chelmus, C. Bonzon, C. Maissen, G. Scalari, M. Beck, and J. Faist, "Subcycle measurement of intensity correlations in the terahertz frequency range," Phys. Rev. A **93**(4), 043812 (2016).
19. C. Riek, D. V. Seletskiy, A. S. Moskalenko, J. F. Schmidt, P. Krauspe, S. Eckart, S. Eggert, G. Burkard, and A. Leitenstorfer, "Direct sampling of electric-field vacuum fluctuations," Science **350**(6259), 420–423 (2015).
20. C. Riek, P. Sulzer, M. Seeger, A. S. Moskalenko, G. Burkard, D. V. Seletskiy, and A. Leitenstorfer, "Subcycle quantum electrodynamics," Nature **541**(7637), 376–379 (2017).
21. H. J. Bakker, G. C. Cho, H. Kurz, Q. Wu, and X.-C. Zhang, "Distortion of terahertz pulses in electro-optic sampling," J. Opt. Soc. Am. B **15**(6), 1795–1801 (1998).
22. M. Knorr, J. Raab, M. Tauer, P. Merkl, D. Peller, E. Wittmann, E. Riedle, C. Lange, and R. Huber, "Phase-locked multi-terahertz electric fields exceeding 13 MV/cm at a 190 kHz repetition rate," Opt. Lett. **42**(21), 4367–4370 (2017).
23. Q. H. Wang, K. Kalantar-Zadeh, A. Kis, J. N. Coleman, and M. S. Strano, "Electronics and optoelectronics of two-dimensional transition metal dichalcogenides," Nat. Nanotechnol. **7**(11), 699–712 (2012).
24. F. Xia, H. Wang, D. Xiao, M. Dubey, and A. Ramasubramaniam, "Two-dimensional material nanophotonics," Nat. Photonics **8**(12), 899–907 (2014).
25. K. S. Novoselov, D. Jiang, F. Schedin, T. J. Booth, V. V. Khotkevich, S. V. Morozov, and A. K. Geim, "Two-dimensional atomic crystals," Proc. Natl. Acad. Sci. U.S.A. **102**(30), 10451–10453 (2005).
26. A. K. Geim and I. V. Grigorieva, "Van der Waals heterostructures," Nature **499**(7459), 419–425 (2013).
27. L. Britnell, R. M. Ribeiro, A. Eckmann, R. Jalil, B. D. Belle, A. Mishchenko, Y.-J. Kim, R. V. Gorbachev, T. Georgiou, S. V. Morozov, A. N. Grigorenko, A. K. Geim, C. Casiraghi, A. H. Castro Neto, and K. S. Novoselov, "Strong light-matter interactions in heterostructures of atomically thin films," Science **340**(6138), 1311–1314 (2013).
28. K. S. Novoselov, A. Mishchenko, A. Carvalho, and A. H. Castro Neto, "2D materials and van der Waals heterostructures," Science **353**(6298), aac9439 (2016).
29. R. A. Kaindl, F. Eickemeyer, M. Woerner, and T. Elsaesser, "Broadband phase-matched difference frequency mixing of femtosecond pulses in GaSe. Experiment and theory," Appl. Phys. Lett. **75**(8), 1060–1062 (1999).
30. R. Huber, F. Adler, A. Leitenstorfer, M. Beutter, P. Baum, and E. Riedle, "12-fs pulses from a continuous-wave-pumped 200-nJ Ti:sapphire amplifier at a variable repetition rate as high as 4 MHz," Opt. Lett. **28**(21), 2118–2120 (2003).
31. D. F. Edwards and H. R. Philipp, "Cubic Carbon (Diamond)," in *Handbook of Optical Constants of Solids*, E. D. Palik, ed. (Academic, 1986).
32. K. Kato, F. Tanno, and N. Umemura, "Sellmeier and thermo-optic dispersion formulas for GaSe (Revisited)," Appl. Opt. **52**(11), 2325–2328 (2013).

Few-cycle pulses with frequencies in the multi-terahertz (THz) and infrared regime have enabled the resonant time-domain observation and control of fundamental low-energy excitations in condensed matter [1–3]. A key asset of THz science and technology has been given by the availability of ultrabroadband electro-optic sensors, which directly map the complete waveform of phase-stable pulses with absolute amplitude and phase, like an oscilloscope for light [4–13]. This technology has made dynamics in molecules and solids accessible on timescales faster than a single oscillation cycle of light [14,15]. Latest advances in lightwave electronics utilizing the carrier wave of THz and infrared pulses as AC bias fields have also benefitted from field-sensitive detection [16]. Shot-noise limited electro-optic sensors have detected coherent THz fields consisting of less than one THz photon per pulse [17,18] or pure quantum fluctuations of the vacuum [19,20], while the detection bandwidth has been systematically extended from the few-THz window to the mid- and near-infrared regime [4–10,12]. Such multi-octave spanning detection bandwidths require exceptionally broadband phase matching between the THz waves and the gate pulses, which typically implies interaction lengths on the order of a few microns or less. Free-standing detection crystals of such low thickness are mechanically unstable in most cases. Furthermore, the large surface-to-volume ratio entails increased chemical reactivity and lower damage thresholds – a critical disadvantage in the pursuit of increased signal-to-noise ratios achievable with shot-noise-limited detection. Finally, optical reflections in short detection crystals occur with ultrashort delays between successive pulse replicas, leading to etalon effects that render a retrieval of the actual waveform difficult [21].

Optics EXPRESS

One way to circumvent these problems is to contact a thin detector crystal to an optically inactive substrate of the same material, enabling perfect refractive index matching. In this context, ZnTe has been an interesting candidate [6] since different crystal orientations can be chosen for the role of the inactive substrate and the active detector. However, ZnTe shows a significantly lower phase-matching bandwidth than other state-of-the-art materials [8]. Furthermore, the typical quality of polished ZnTe surfaces makes the fabrication of a gap-free optical contact challenging and the detectors prone to residual reflections. A conceptually different approach based on thick detection crystals exploits the fact that, for broadband gate pulses, different spectral components average out rapid phase-matching oscillations [10]. While this scheme enables broadband detection, the obtained sensitivities are lower than what is obtained using thin ZnTe crystals. Furthermore, the precise correction for the detector-dependent response function remains a critical challenge.

In the meantime, there has been an ongoing revolution in the field of van-der-Waals layered crystals [23–25]. Owing to their strong in-plane and weak interlayer bonding, these chemically inert materials can be readily exfoliated to various thicknesses, even down to the monolayer limit [25]. Van-der-Waals bonding also facilitates the deterministic preparation of atomically clean interfaces between different materials and complex heterostructures by mechanically contacting thin crystalline flakes, opening unforeseen possibilities to tailor electronic and optical material properties [26–28]. A promising representative in the class of van-der-Waals layered materials is gallium selenide, which has been shown to be highly suitable for ultrabroadband generation and detection of multi-THz pulses because of its high electro-optic coefficient as well as its large phase-matching bandwidth [7–9,29].

Here, we merge the advantages of van-der-Waals layered materials with electro-optic sampling and present highly sensitive ultrabroadband detection of multi-THz waveforms while simultaneously suppressing early reflections to relative intensities below 2×10^{-3}. To this end, we optically contact thin GaSe flakes to a thick diamond substrate, combining an efficient electro-optic detector with an optically robust substrate. The straightforward and cost-effective fabrication process results in high-quality mm^2-sized detectors of excellent lateral homogeneity and high optical damage thresholds. The phase response of this detector deviates from a linear profile by less than $\pi/20$ over the spectral window from 10 THz to 150 THz, eliminating phase-dependent distortions of the detected THz waveforms.

Figure 1(a) depicts a typical electro-optic sampling setup, where a phase-locked multi-THz or infrared waveform is focused into an electro-optic crystal. The electric carrier field induces a transient birefringence, which is translated into a polarization change of a co-propagating ultrashort gating pulse. After a quarter-wave plate, this change in polarization manifests itself in an elliptical deviation of the otherwise circular gate polarization, which is directly proportional to the instantaneous electric field. This effect is read out by a combination of a Wollaston prism and balanced photodiodes. The full waveform can be reconstructed in amplitude and phase by varying the delay between the multi-THz pulse and the gate. Since the multi-THz pulse is partially reflected at the end facets of the crystal and thus traverses the crystal again, the electro-optic trace is distorted by multiple reflection echoes trailing the main pulse (Fig. 1(a), inset). Reflections of the gate pulse, in turn, lead to precursors. For very thin crystals, such reflections overlap with the main pulse, which further complicates the recovery of the actual incident waveform. To achieve longer reflection-free temporal windows, thicker crystals are thus required.

Optics EXPRESS

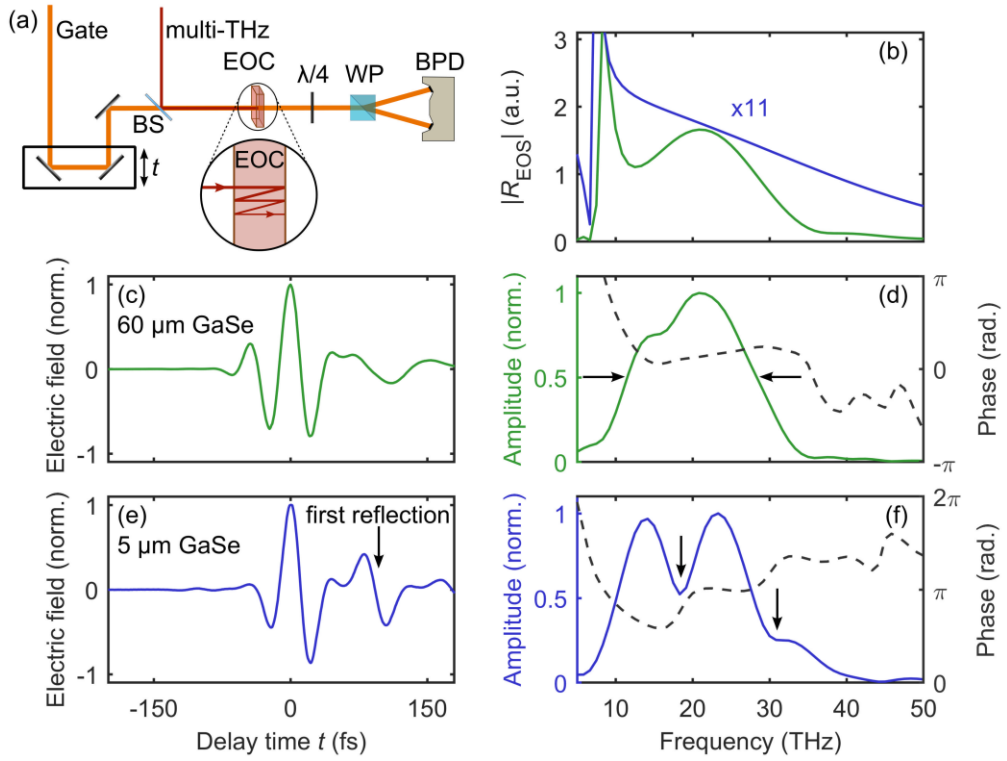

Fig. 1. Typical limitations in electro-optic detection of few-cycle THz transients. (a) Setup for electro-optic detection. BS, beam splitter; EOC, electro-optic crystal; λ/4, quarter-wave plate; WP, Wollaston prism; BPD, balanced photodiodes. (b) Amplitude response function $|R_{EOS}|$ of a 5-µm-thick (blue) and a 60-µm-thick (green) GaSe electro-optic sensor with optimal phase matching for a gate pulse centered at 800 nm with a bandwidth-limited duration of 12 fs. (c) Electro-optic trace as measured with a 60-µm-thick GaSe crystal at an external phase matching angle of θ = 50°. (d) Corresponding amplitude spectrum of the transient shown in (c). The bandwidth (FWHM, black arrows) is limited by the detector response. (e) Same THz transient as detected in a 5-µm-thick crystal at the same phase matching angle. The first reflection occurs at a delay time of 82 fs and leads to spectral interference effects (black arrows) in the frequency domain (f).

Electro-optic detection may also be understood as phase-matched sum and difference frequency mixing between the THz and the gate pulses [6]. Recording single-cycle field transients with multi-octave spanning spectra requires ultrabroad phase-matching bandwidths, which call for extremely thin electro-optic crystals. This requirement, however, conflicts with the quest for thicker crystals to prevent early echoes.

This situation is exemplified in Fig. 1, where we compare the detection of a reference multi-THz transient in GaSe crystals of thicknesses of 60 µm and 5 µm, respectively. The reference transient is generated by optical rectification of a near-infrared pulse from a Ti:sapphire amplifier (center wavelength: 800 nm, pulse duration: 12 fs, repetition rate: 400 kHz) [30] in an 18-µm-thick GaSe crystal. Another portion of the laser output is used as a gate for electro-optic sampling. For the gate pulse used, phase matching limits the bandwidth of the calculated amplitude response function of the 60-µm-thick GaSe sensor to a FWHM of 22 THz, while the response function of the 5-µm crystal remains fairly flat between 10 and 50 THz (Fig. 1(b)).

In fact, the experimental waveform recorded with the 60-µm sensor (Fig. 1(c)) shows an additional oscillation half-cycle as compared to the transient obtained with the 5-µm detector

Optics EXPRESS

(Fig. 1(e)). Even though the phase matching of the thicker sensor is adjusted to the center frequency of the multi-THz transients, the measured spectrum is still limited by the phase-matching bandwidth (Fig. 1(d)). Since critical phase matching depends on the azimuthal tilt of the crystal, slight misalignment may strongly affect the apparent waveform. The thin detector crystal, in turn, enables sufficiently broadband phase matching for single-cycle THz detection that is rather insensitive to misalignment. However, the first reflection of the THz pulse occurs already at a delay time of 82 fs (Fig. 1(e), black arrow), limiting the useful time window for pump-probe measurements and leading to strong Fabry–Perot interference effects in the spectral domain (Fig. 1(f)). In addition, reflection of the gate pulse causes slight oscillations of the electro-optic signal at negative delay times.

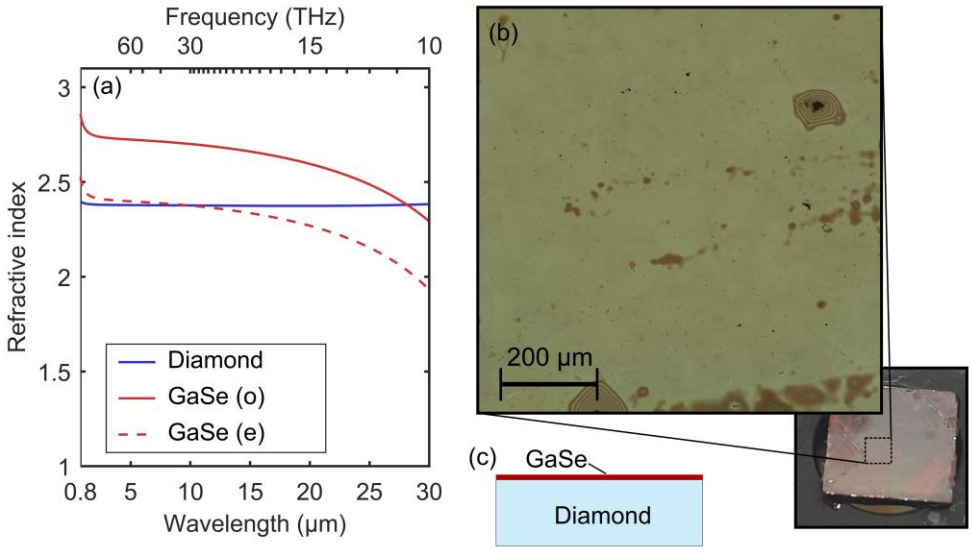

Fig. 2. Refractive index of the diamond substrate [31] and principal values of the refractive index of the GaSe detector for ordinary (o) and extraordinary (e) polarization [32]. (b) Optical microscope image and photograph (bottom right) of the GaSe flake contacted to the diamond substrate via van-der-Waals interaction. Dark spots in the microscope image correspond to areas with imperfect adhesion, while lighter-colored areas indicate excellent optical contact. (c) Schematic side view of the new detector.

We resolve these issues by contacting thin GaSe flakes to a suitable index-matched substrate via van-der-Waals bonding. Diamond is an ideal candidate for this purpose. Its refractive index, which also matches most transition metal dichalcogenides, differs from the value of GaSe by less than 0.3 over the entire multi-THz range (Fig. 2(a)). Therefore, the reflectivity of the GaSe-diamond interface (0.5%) for an s-polarized THz pulse incident under a phase-matching angle of $\theta = 50°$ is reduced by almost two orders of magnitude as compared to the bare GaSe-air interface (36%). Furthermore, diamond is mechanically robust and chemically inert. It features a high thermal conductivity and its large bandgap suppresses substrate-induced distortions of the measured transient waveform caused by linear absorption or nonlinearities.

We fabricate our structures by mechanically exfoliating thin flakes of GaSe with a tape and gently pushing them onto a CVD-grown polycrystalline diamond substrate pre-wetted with methanol. Evaporation of excess methanol establishes a high-grade van-der-Waals contact over large areas on the scale of 1 mm^2 as shown by the transmission microscope image of a 5-μm-thick GaSe flake optically contacted to a 500-μm-thick diamond substrate (Fig. 2(b)). The presence of optical interference fringes surrounding a few isolated impurities attests to the otherwise excellent contact on optical scales.

Optics EXPRESS

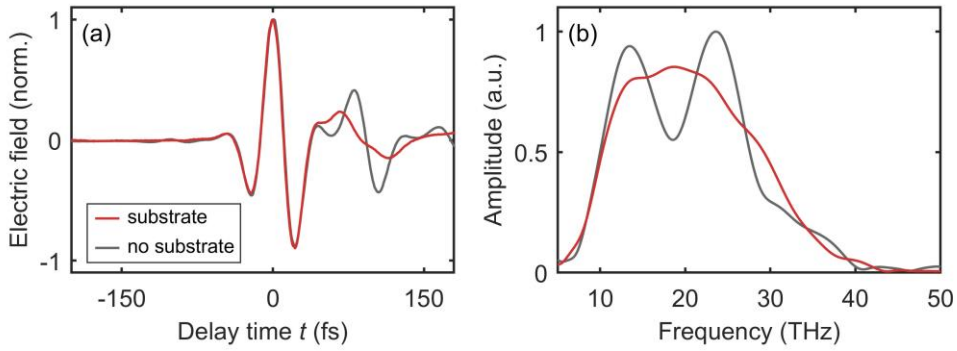

Fig. 3. (a) Multi-THz transient electro-optically detected by our optically contacted, 5-µm-thick GaSe crystal (red curve). The transient obtained by a free-standing GaSe flake is shown for reference (grey curve). (b) Corresponding etalon-free (red curve) and modulated amplitude spectrum (grey curve).

We test our new detector by electro-optic sampling of the single-cycle multi-THz waveform recorded in Fig. 1. To avoid that dispersion in the diamond substrate affects the nonlinear optical interaction between the THz and the gate pulses, they traverse the GaSe active detector layer first. Moreover, potential gate-induced photoconductivity is negligible for the moderate energy of the gate pulse (pulse energy: 25 nJ) and the high multi-THz frequencies of interest. Figure 3(a) compares the electro-optic signal as detected with a 5-µm-thick free-standing (Fig. 3(a), grey curve) and diamond contacted (Fig. 3(a), red curve) sensor. The refractive index matching between GaSe and diamond suppresses both the reflection of the multi-THz transient at a delay time of t = 82 fs, as well as the reflection of the gate pulse, seen at t = –95 fs, corroborating the excellent optical contact between sensor and substrate. The first reflection caused by the detector system now appears after 8 ps, corresponding to the 500 µm thickness of the substrate (not shown). This window can be easily increased by choosing thicker substrates. The recorded spectrum (Fig. 3(b)) displays a full width at half maximum of 20 THz with a center frequency of 19 THz and only slight residual modulations in the spectrum.

In the past, intense efforts have been made to retrieve the actual transient field from the measured electro-optic waveform by correction for the detector response R_{EOS} [10,21]. For a multi-THz frequency Ω and a gating pulse spectrum $E_g(\omega)$ one finds [10]:

$$R_{EOS}(\Omega) \sim \int_{\omega>\Omega} d\omega\, E_g^*(\omega) E_g(\omega-\Omega) \chi^{(2)}(\omega,\Omega) \frac{\omega^2}{k(\omega)} T(\omega,\Omega) P(\omega,\Omega,L), \quad (1)$$

where $\chi^{(2)}(\omega,\Omega)$ denotes the second order susceptibility for electro-optic detection, $k(\omega)$ represents the wave vector, $T(\omega,\Omega)$ accounts for Fresnel transmission through the crystal front facet, and $P(\omega,\Omega,L)$ describes phase matching, which is directly dependent on the crystal length L:

$$P(\omega,\Omega,L) = \frac{\exp(i\,\Delta k\, L) - 1}{\Delta k}, \quad (2)$$

with the wave-vector mismatch Δk. For ultrabroadband detection, the bandwidth-limited gate pulse needs to be extremely short, such that the overlap of the gate spectrum $E_g(\omega)$ with the difference frequency component $E_g(\omega - \Omega)$ remains high, even at large multi-THz frequencies Ω (see Eq. (1)).

We calculate the response function for GaSe and ZnTe crystals of various thicknesses for two different unchirped gate pulse spectra $E_g(\omega)$ corresponding to pulse durations of 12 fs and

Optics EXPRESS

5 fs, respectively (Figs. 4(a) and 4(b)). For phase-matched propagation, the amplitude response of GaSe crystals as thin as 5 µm exceeds the response of both thin and thick ZnTe crystals by more than one order of magnitude over the entire spectral range. While a 7-µm-thick ZnTe sensor shows a negative slope in the phase between 60 and 75 THz due to a minimum in the phase-matching curve located at a frequency of 66 THz, there is no such minimum with the new detector for frequencies between 10 and 150 THz. Instead the phase response in this region is linear within a margin of π/20, corresponding to a pure temporal shift of the detected transient with respect to the actual waveform. Remarkably, we find that the bandwidth of the EOS response function is not mainly limited by phase-matching inside the crystal. Instead the duration of the gate pulse limits the detection efficiency at high multi-THz frequencies for typically available sampling pulses with durations of 5 fs and above. For 5 fs gate pulses, the amplitude of the EOS response function varies by less than a factor of 1.7 over the whole spectral range between 10 and 50 THz. In contrast, the amplitude of the response function changes by a factor of 5 in the same range, for both the 7-µm-thick and the 300-µm-thick ZnTe crystals and the same gate pulse duration of 5 fs.

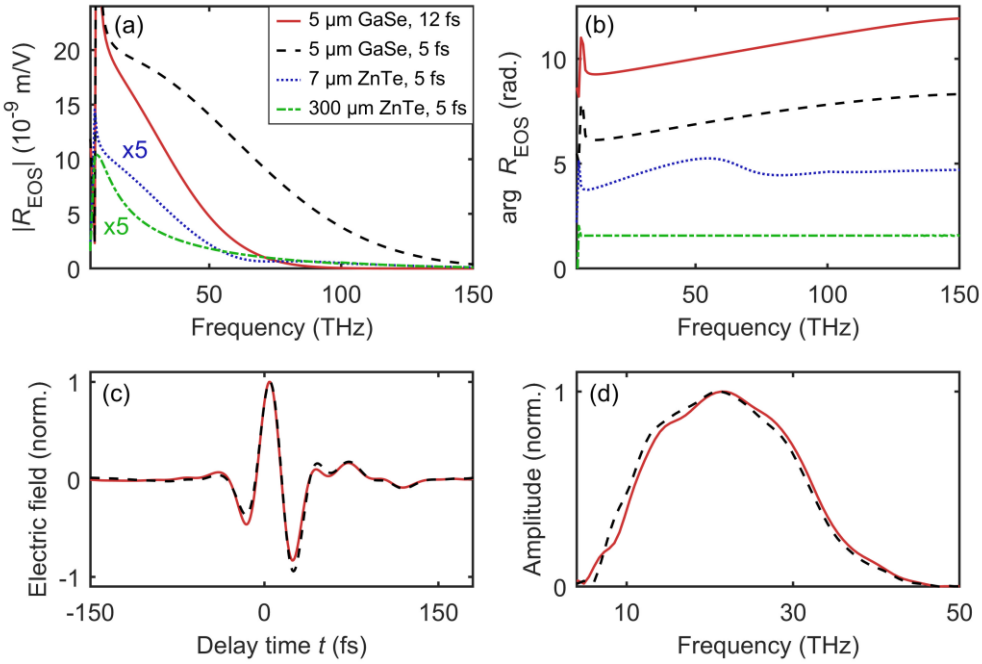

Fig. 4. (a) Absolute value and (b) phase of the EOS response function R_{EOS} for ZnTe and GaSe crystals of different crystal thicknesses and for different gate pulse durations. The red curves indicate the response function of the detector used in the experiment of Fig. 3. Phase spectra are vertically offset for clarity. (c) Incident electric field retrieved from the transient of Fig. 3(a) through correction for the experimental detector response (red). Black dashed line: Expected electro-optic waveform as it would be detected with a diamond-contacted GaSe sensor of a thickness of 5 µm and a 5 fs gate pulse. (d) Corresponding amplitude spectra retrieved through Fourier transform of the data shown in (c).

Figure 4(c) compares the electro-optic trace (dashed line) of a multi-THz transient (red line) as one would expect to measure it with a 5-µm-thick diamond-contacted GaSe detector and a 5 fs gate pulse. The excellent agreement of the measured and the incident waveforms (Fig. 4(c)) and their corresponding spectra (Fig. 4(d)) renders direct in situ measurement of the actual transient waveform possible, even without correction for the EOS response function.

Optics EXPRESS

In conclusion, we report on a new type of detector for ultrabroadband electro-optic sampling. When contacting thin flakes of the van-der-Waals layered material GaSe to a diamond substrate, the matching of the refractive indices of the two materials suppresses reflections of the multi-THz and gate pulses, opening up an 8 ps reflection-free time window. The use of an easy-to-prepare thin GaSe crystal on a diamond substrate has decisive advantages over previous ZnTe- and GaP-based electro-optic detectors, such as a higher electro-optic coefficient and broader phase-matching bandwidths, even enabling the measurement of the true transient field without correction for the detector response. Since electro-optic sampling is the inverse quantum process of optical rectification, we also anticipate that the new van-der-Waals contacted layered semiconductors will enable robust emitters of sub-cycle mid-infrared fields with unprecedented bandwidths. Finally, custom-tailored heterostructures of van-der-Waals layered materials in combination with index-matched substrates may allow for novel applications in the entire field of optoelectronics including etalon-free ultrabroadband electro-optic sampling up to the attosecond regime.

Funding

European Union FET-Open grant (737017) MIR-BOSE

Acknowledgments

We thank Thomas Maag for helpful discussions.